Power-Law Spectra of Incipient Gas-Curtain Turbulence

Peter Vorobieff,[1,2] Paul M. Rightley,[2] and Robert F. Benjamin[2]
[1]*Center for Nonlinear Studies, Los Alamos National Laboratory, Los Alamos, New Mexico, 87545*
[2]*Dynamic Experimentation Division, Los Alamos National Laboratory, Los Alamos, New Mexico, 87545*
(Received 17 April 1998)

We investigate the evolution of a thin curtain of heavy gas (SF_6) embedded in a lighter gas (air) and accelerated with a Mach 1.2 planar shock wave. The Richtmyer-Meshkov instability leads to growth of the initial perturbations of the curtain and eventually to transition to turbulence. We visualize a time sequence of images of a section of the flow illuminated with a laser sheet. The SF_6 is premixed with tracer (glycol fog), so the intensity of the light scattered off the curtain grows with the local density. As the curtain evolves towards a fully mixed state, real-space correlations of the density, inferred from scattered light intensity, show the emergence of a power-law behavior, indicative of transition to turbulence. [S0031-9007(98)07098-7]

PACS numbers: 47.27.Cn, 47.20.Ma, 47.40.Nm

The problem of transition to turbulence is a very general one. A unified theory describing it has yet to be developed, and to date, experimental and numerical studies of the transition by no means present a complete phenomenological picture. Clear, quantitative experimental results are particularly scarce.

This Letter describes an experimental study of transition to turbulence due to Richtmyer-Meshkov (RM) instability. RM is the shock-accelerated analog of the more widely known Rayleigh-Taylor instability driven by constant acceleration. As the shock wave passes through a density interface, it produces vorticity wherever the shock front is not parallel to the interface. Vortices forming on the interface dominate the instability growth after its initial linear stage. After a period of nonlinear vortex-dominated growth, secondary instabilities produce disordered features on multiple scales, leading to the onset of turbulence.

The RM instability serves as a useful test problem for the studies of transition to turbulence, because the RM-unstable interface "coasts" after the initial acceleration, whereas the growth of an RT-unstable interface is continuously driven by gravity. Thus RM instability has smaller growth rates, simplifying the investigation of the transition interval.

RM instability, in particular, the linear and vortex-dominated stages, has been the topic of experimental [1–4] and numerical [5,6] studies, as well as subject to theoretical treatment [7,8]. The instability growth in the turbulent regime has also been examined [9]. Some of these studies describe the evolution of a single interface [5,7–9]; some consider the situation when a gas curtain is formed by two nearby interfaces [1–4,6].

Nonetheless, the process of the *transition* to turbulence has not been investigated thoroughly, despite its importance for a large number of applications, their scope ranging from microscopic to astrophysical. Evidence of this transition due to RM instability in both single-interface and gas curtain experiments was largely phenomenological. Some quantitative gas-curtain measurements of mixing (histogram analysis) and scale evolution (wavelet transform) were produced recently [10]. This Letter offers new quantitative results in a form more easily comparable with the well-known statistical theories of fully developed homogeneous incompressible turbulence.

We present statistical evidence of the transition to turbulence in a thin curtain of heavy gas (SF_6) embedded in a lighter gas (air) and accelerated by a planar shock (Mach 1.2) in a horizontal shock tube. We analyze sequences of instantaneous images acquired by illuminating the curtain with a laser sheet, and produce second-order structure functions of the intensity of light scattered off the curtain material. Structure functions have been extensively employed to characterize fully developed turbulent flows. In fact, the original 1941 formulation of Kolmogorov turbulence theory [11] was made in terms of structure functions of velocity rather than in terms of Fourier spectra of kinetic energy. The second-order structure function of intensity can also be regarded as the intensity-intensity correlation. Our results for the cases with the strongly perturbed initial conditions show the second-order structure functions evolving towards a power-law behavior consistent with the $k^{-5/3}$ scaling of the density spectra. These results agree with several other works observing a similar scaling, as well as with the recent theory. We present a detailed evolution analysis for the exponent of the second-order structure function of density. For RT instability, results similar to ours have been reported [12]. This similarity, as well as the similarity between the gas-curtain "mixing transition" we observe [10] and the mixing transition in shear layers [13,14], suggests general traits of transition to turbulence independent of the details of the transition mechanism. These results indicate that the scaling predicted and observed for fully developed, isotropic and homogeneous turbulence emerges in strongly nonisotropic and inhomogeneous transitional flows.

The layout of the experiment is shown in Fig. 1. The curtain is formed by injecting SF_6 premixed with a small

 0031-9007/98/81(11)/2240(4)$15.00

($<10^{-6}$) volume fraction of glycol fog (droplet size $<0.5\ \mu$m) into the top of the test section of the shock tube through a varicose nozzle. A horizontal section of the curtain is illuminated with a thin (2 mm) laser sheet. The glycol fog is a reliable tracer, and the intensity of laser light scattered off the droplets serves as a good indicator of the local concentration of the curtain material [4]. The initial cross section of the curtain is imposed by the varicose shape of the injection nozzle. The curtain material is actively removed at the bottom of the test section. Pressure transducers trigger a gated, intensified CCD camera as the shock approaches the test section, leaving multiple images of the evolving curtain on the CCD as the curtain is carried downstream after shock acceleration. The images record the initial condition of the curtain and up to eight subsequent dynamic exposures, showing several distinct flow morphologies that evolve [4,10].

This experimental setup offers several advantages for the study of transition to turbulence. The initial geometry of the curtain determines the structure of the vorticity field produced after the shock interaction. A spatially regular varicose cross section imposed on the curtain produces a row of counterrotating vortices that drive the nonlinear growth of the curtain. Small variations in the shape of the curtain from experiment to experiment produce a variety of initial conditions, while the initially regular structure of the flow makes it possible to concentrate the analysis on the growth of stochastic features.

Figures 2a and 2b show two image sequences acquired as described in Ref. [4]. The direction of the shock is from left to right, the vertical extent of each image is 35 mm, and the perturbation wavelength imposed on the curtain by the varicose nozzle is $\lambda = 6$ mm. The first image from the left is the initial condition, the second image from the left is the first dynamic exposure (about 60 μs after the shock), and the intervals between the following dynamic exposures are 60, 80, 80, 120, 120, 120, and 120 μs. Labels in Fig. 2 show time nondimensionalized by the combination of piston velocity ($U \simeq 100$ m/s) and the fundamental wavelength λ. This dimensionless time can also be interpreted as downstream distance in units of λ traveled by the perturbed curtain.

The initial perturbation in the first image sequence (Fig. 2a) has a moderate amplitude ($\sim 0.25\lambda$) and a regular varicose shape. In this case, alternating concentrations of positive and negative vorticity are deposited along the extent of the curtain, and the shock interaction causes phase inversion of the downstream interface of the curtain. As the vortex pairs roll up the curtain material, the curtain retains a regular, sinuous structure, eventually developing into a row of mushroom shapes facing upstream and downstream—the evolution pattern labeled "sinuous mode" in the previous studies. In Fig. 2b, the pattern known as "multimode" is presented. This flow pattern evolves from strongly perturbed initial conditions (amplitude $\sim 0.45\lambda$). Strong mixing of the curtain material with air is apparent at late stages, as is the presence of numerous small-scale structures in the flow.

Results of the quantitative analysis of the images follow. We plot the second-order structure function of the intensity I of the light scattered off the curtain, $I_2(r) = \langle [I(\mathbf{x} + \mathbf{r}) - I(\mathbf{x})]^2 \rangle$, where $\langle \cdot \rangle$ denotes spatial averaging in the image plane for all points $\mathbf{x} = (x, y)$ and all 2D radius vectors $\mathbf{r}, |\mathbf{r}| < 1.5\lambda$. Intensity I is proportional to the local density ρ of the curtain material (with the maximum value corresponding to 60% SF_6). The visually noticeable nonuniformity in the intensity of the laser sheet in Fig. 2 does not exert any systematic influence on the structure functions within the scale range we investigate ($r < 1.5\lambda$), as the characteristic scale of this nonuniformity is approximately four fundamental wavelengths. Analysis is carried out in real space rather than Fourier space because the resolution of our digital images is modest (typically 120×400 per dynamic exposure). Thus we avoid problems that might arise from windowing effects.

Figures 3 and 4 show $I_2(r)$ for the initial conditions, first, fifth, and eighth dynamic exposures for the images shown in Figs. 2a and 2b, respectively. The corresponding dimensionless exposure timings are $tU/\lambda = 0$, 0.77, 6.43, and 12.43 for Fig. 2a and $tU/\lambda = 0$, 0.93, 6.67, and 12.60 for Fig. 2b.

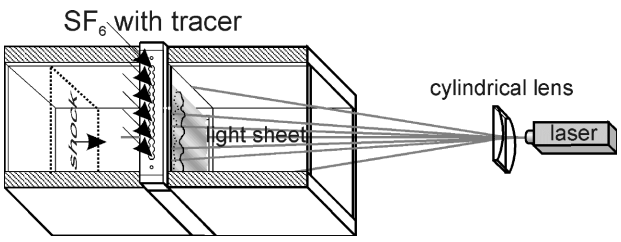

FIG. 1. Schematics of the experimental setup: Test section of the shock tube.

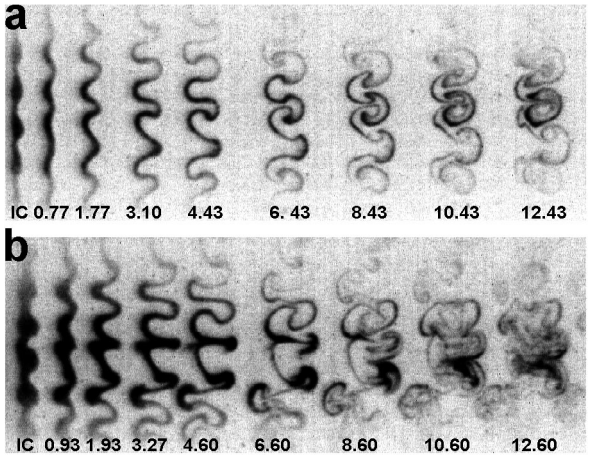

FIG. 2. Sinuous (a) and multimode (b) curtain evolution patterns. "IC" marks initial conditions. Dimensionless exposure timings in the figures are described in the text.

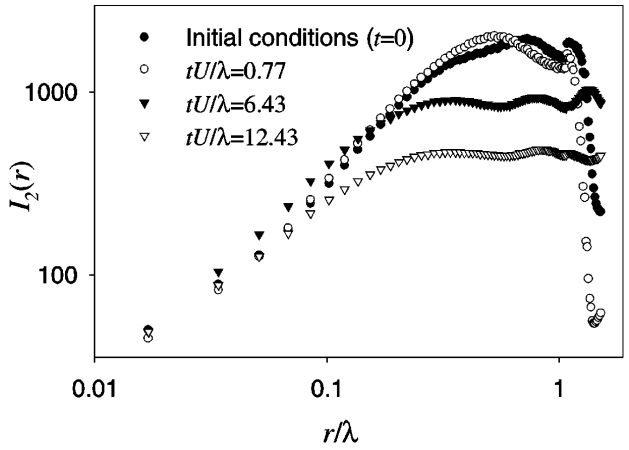

FIG. 3. Second-order structure function I_2: Sinuous mode flow pattern, Fig. 2a.

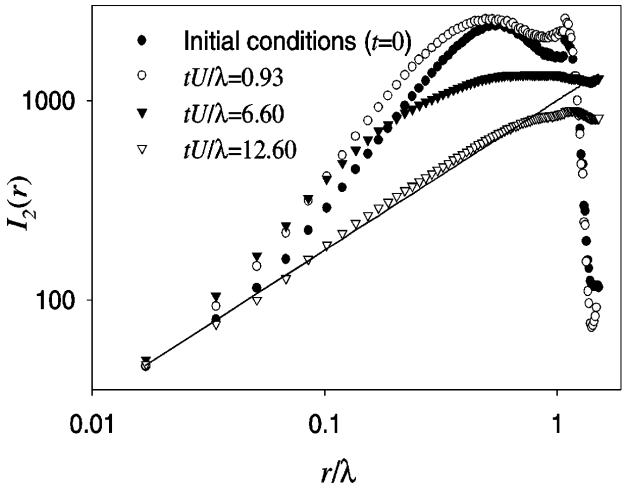

FIG. 4. Second-order structure function I_2: Multimode flow pattern, Fig. 2b. The solid line indicates exponent 0.73.

The initial conditions in both cases show peaks at $r = \lambda$ and at $r \sim 0.6\lambda$. The second peak matches the size of "bulges" in the initially varicose shape of the curtain. After the phase inversion following the shock interaction, it moves to $r \sim \lambda/2$—the scale of the developing "mushroom caps." The peaks are somewhat sharper for the more regular initial conditions in Fig. 2a, but qualitatively the structure functions of the initial conditions and first dynamic exposure show no other difference. As the flow evolves, however, the differences become apparent, in particular, in the range $0.1 < r/\lambda < 0.6$. For the sinuous mode, the fifth dynamic exposure plot ($tU/\lambda = 6.43$) shows several peaks associated with the initial wavelength λ and scales of the mushrooms: 0.3λ and 0.7λ. These well-defined peaks are not present in the corresponding plot for the multimode flow morphology ($tU/\lambda = 6.60$). In the eighth dynamic exposure plot for the sinuous mode ($tU/\lambda = 12.43$), the peaks associated with the mushrooms are still present. In contrast, the multimode morphology plot ($tU/\lambda = 12.60$) shows monotonic power-law-like behavior over the extent of about 1.6 decades in r/λ, with an exponent 0.73. This would translate into a -1.73 power law in wave number space. Visual comparison of the last dynamic exposures in Figs. 2a and 2b reveals persistence of the regular flow structure for the sinuous mode and apparent turbulence in the multimode case.

We analyzed four other multimode morphology images with apparent strong mixing at late times. For all of these, the second-order structure functions of intensity of the final dynamic exposure show similar features. Over more than a decade in r, their behavior is consistent with power law, the exponents being 0.70 ± 0.04.

Can this result be compared with theory? The scaling of velocity power spectra has been studied extensively, and numerous experimental confirmations of the Kolmogorov $k^{-5/3}$ power law exist—to the extent that observation of such scaling is often considered to be a signature of fully developed incompressible turbulence. One must note, however, that the shapes of amplitude spectra are only weakly related with the spatial structure of the flow [15]. As pertains to density power spectra, much less information is available both from theory and experiment. The $-5/3$ scaling characterizes the spectra of the concentration of a passive scalar advected by homogeneous turbulent flow [16,17]. The recent work [18] on stochastic interpretation of fluid mechanics, as well as some theories applied to astrophysical observations [19,20], give the same scaling exponent for density spectra. So do experimental measurements in turbulent wakes [21] and the recent study of explosively driven flows with density variations [22]. The latter case does not involve fully developed homogeneous turbulence. Emergence of $-5/3$ exponent has also been observed in the evolution of Rayleigh-Taylor instability [12]. Thus the $-5/3$ scaling may apply to a wider scale of phenomena than just homogeneous, isotropic, fully developed Kolmogorov turbulence. It must also be mentioned that, while our results are consistent with the $-5/3$ scaling, other theoretical predictions (e.g., the -1 scaling or the exponential decay suggested by Batchelor [23]) would be inconsistent with these results.

Also of interest is the evolution of the exponent of a power-law fit applied to the structure functions in the range $r/\lambda < 0.3$, corresponding to scales smaller than the characteristic scale of the regular structures. Figure 5 shows the exponents and errors of such fits applied to the images in Fig. 2. In both cases, the exponent is close to 1.4 at early times and approaches 0.7 at late times. However, the transient behavior is different, with the multimode morphology exponent reaching the minimal value after the fifth dynamic exposure ($tU/\lambda = 6.60$). In the sinuous morphology case, the exponent approaches 0.7 slower and the error of the fit does not decrease as much as it does for the multimode case. The duration of the experiment may be too short an interval for the regular morphology to develop a sufficient amount of

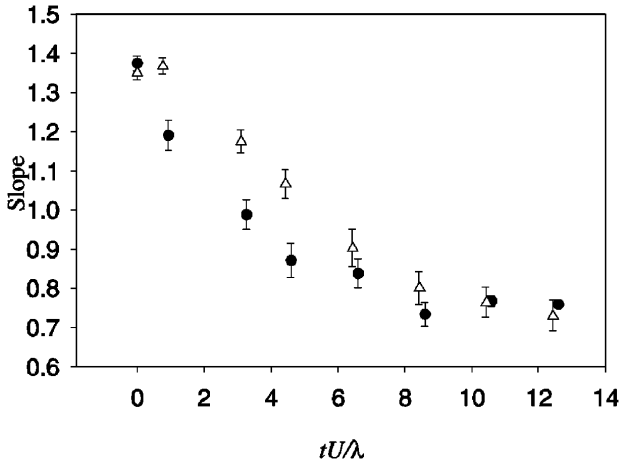

FIG. 5. Slopes and errors (error bars) of a power-law fit of second-order structure functions of intensity for images shown in Fig. 2. △: sinuous morphology (Fig. 2a); •: multimode morphology (Fig. 2b). Fit applies to $r/\lambda < 0.3$.

disordered structures and evolve to a true power-law behavior. These results are consistent with our previous study [10], analyzing the gas-curtain data by histogram and wavelet analysis. When the shock accelerates the curtain, strongly perturbed multimode initial conditions produce more vorticity than the sinuous case, and this vorticity is more disordered. As a consequence, the mixing transition (an abrupt acceleration of mixing) occurs at $tU/\lambda = 6.60$ for the multimode morphology (Fig. 2b), while no such transition is observed for the sinuous morphology (Fig. 2a). This transition occurs simultaneously with the change in the behavior of the power-law fit exponent (with a 120 μs temporal accuracy due to late-time interexposure interval).

Our study of the later stages of the evolution of a heavy gas curtain embedded in air and accelerated with a shock wave can be summarized as follows. Our diagnostic [4] produces multiple images of an evolving section of the curtain. For each of these images, we plot second-order structure functions of the curtain material concentration. We present such plots for regular and multimode flow morphologies. As the curtain evolves towards a fully mixed state, the structure functions approach a power-law behavior with an exponent close to $2/3$, which would correspond to $-5/3$ slope for Fourier density spectra characteristic of fully developed turbulence. The evolution is faster for the flow morphologies evolving from initial conditions with stronger multimode perturbations. The structure function behavior approaches $2/3$ power law simultaneously with the mixing transition occurring in the curtain.

We acknowledge the support of the U.S. Department of Energy for this work. We thank Robert E. Ecke, Robert A. Pelak, William J. Rider, and Timothy T. Clark for their suggestions on the manuscript. We are grateful to Frank Kosel and Hadland Photonics, Ltd. for use of their SVR digital camera.

[1] J. W. Jacobs, D. L. Klein, D. G. Jenkins, and R. F. Benjamin, Phys. Rev. Lett. **70**, 583 (1993).
[2] J. M. Budzinski, R. F. Benjamin, and J. W. Jacobs, Phys. Fluids **6**, 3510 (1994).
[3] J. W. Jacobs, D. G. Jenkins, D. L. Klein, and R. F. Benjamin, J. Fluid Mech. **295**, 23 (1995).
[4] P. M. Rightley, P. Vorobieff, and R. F. Benjamin, Phys. Fluids **9**, 1770 (1997).
[5] R. L. Holmes, J. W. Grove, and D. H. Sharp, J. Fluid Mech. **301**, 51 (1995).
[6] R. M. Baltrusaitis, M. L. Gittings, R. P. Weaver, R. F. Benjamin, and J. M. Budzinski, Phys. Fluids **8**, 2471 (1996).
[7] J. W. Grove, R. L. Holmes, D. H. Sharp, Y. M. Yang, and Q. Zhang, Phys. Rev. Lett. **73**, 3178 (1994).
[8] A. L. Velikovich and G. Dimonte, Phys. Rev. Lett. **76**, 3112 (1996).
[9] G. Dimonte, C. E. Frerking, and M. Schneider, Phys. Rev. Lett. **74**, 4855 (1995).
[10] P. M. Rightley, P. Vorobieff, and R. F. Benjamin (to be published).
[11] A. N. Kolmogorov, Dokl. Akad. Nauk SSSR **30**, 301 (1941).
[12] S. B. Dalziel, P. F. Linden, and D. L. Youngs, in *Proceedings of the 5th International Workshop on Compressible Turbulent Mixing, Stony Brook, New York, 1995* (World Scientific, Singapore, River Edge, NJ, 1996), p. 321.
[13] L. P. Bernal and A. Roshko, J. Fluid Mech. **170**, 499 (1986).
[14] J. C. Lasheras, J. S. Cho, and T. Maxworthy, J. Fluid Mech. **172**, 231 (1986).
[15] L. Armi and P. Flament, J. Geophys. Res. **90**, 11 779 (1985).
[16] A. M. Obukhov, Izv. Akad. Nauk SSSR **13**, 58 (1949).
[17] S. Corrsin, J. Appl. Phys. **22**, 469 (1951).
[18] M. J. Steinkamp, T. T. Clark, and F. H. Harlow, "Stochastic Interpretation of Fluids," Int. J. Multiph. Flow (to be published).
[19] J. C. Higdon, Astrophys. J. **285**, 109 (1984).
[20] B. J. Bayly, C. D. Levermore, and T. Passot, Phys. Fluids **4**, 945 (1992).
[21] D. Gresillon, G. Gemaux, B. Cabrit, and J. P. Bonnet, Eur. J. Mech. B **9**, 415 (1990).
[22] R. N. Silver, R. Gore, J. Greene, F. Harlow, and R. Whitman, Phys. Rev. Lett. **77**, 2471 (1996).
[23] G. K. Batchelor, J. Fluid Mech. **5**, 113 (1959).